Photocatalysis

DOI: 10.1002/ange.201300239

Gold-Nanorod-Photosensitized Titanium Dioxide with Wide-Range Visible-Light Harvesting Based on Localized Surface Plasmon Resonance**

*Lequan Liu, Shuxin Ouyang, and Jinhua Ye**

In the quest to solve environmental remediation and solar energy conversion issues, photocatalysis using sunlight have been attracting tremendous attention.[1] As a green chemistry technology, photocatalysis is an ambient temperature process that can completely decompose organic pollutants even at low levels.[2] Since the discovery of its photocatalytic activity under UV light,[3] TiO_2 has become the most extensively studied semiconductor in applications such as environmental cleaning and hydrogen energy.[4] Nevertheless, TiO_2 possesses a wide band gap which limits its photo-absorption to only the UV region, accounting for about 4% of the total sunlight. From the perspective of both chemistry and practical applications, it is undoubtedly important to develop photocatalytic materials that harvest a wide range of visible photons. Many strategies, including metal-ion[5] and nonmetal doping,[6] have been proposed to extend the absorption of TiO_2 to visible spectrum. However, to date, the doped materials typically suffer from thermal instability, photocorrosion, and fast e^-/h^+ recombination rates.

The recent and rapid development of localized surface plasmon resonance (LSPR) photosensitization has offered a new opportunity to overcome the limited efficiency of photocatalysts.[7] That is, semiconductors loaded with coinage metals, such as Au, Ag and Cu, exhibited visible-light activity based on LSPR, which has been observed in several photochemical processes.[8] These enhancement effects might be caused by the charge transfer from photoexcited metal to the semiconductor and/or LSPR-induced electromagnetic fields in the vicinity of the plasmonic nanostructure.[7b] From this perspective, in any case, not only improved absorption of photons by LSPR of metal nanoparticles but also a closed interface between metal and semiconductor is important to enhance visible-light activity in plasmonic composite photocatalysts. The presence of an obstacle on the interface, such as surfactant, will hinder the direct charge transfer or dramatically decrease the intensity of LSPR-induced electromagnetic field close to semiconductor, as this field decays exponentially with distance.[9] Calcination is typically the most simple way to remove surfactants, but it could not be easily applied to metal nanoparticles with specific morphology, such as rods, wires, or cubes, which cannot survive in high temperatures. Some efforts were made to coat those nanostructures with semiconductors.[10] Nevertheless, active sites are also masked in this process while surfactant still adheres onto metal nanostructures.[11] On the other hand, among plasmonic composite photocatalysts, tremendous efforts were focused on harvesting visible light around characteristic adsorption of coinage metal nanoparticles (Ag: ca. 410 nm, Au: ca. 520 nm),[7b] while little effort was put into harvesting longer-wavelength visible light which accounts for a larger proportion of solar energy.[12] We report herein a wide-range visible light harvesting of TiO_2 by introducing Au nanorods (NRs) as antennas, while surfactant removal is achieved by an $HClO_4$ oxidative method without any noticeable change in Au NR morphology. It was found that not only transversal plasma which is similar to sphere Au particles, but also longitudinal plasma of Au NRs (with adsorption centered from 630 nm to 810 nm) could induce photocatalytic oxidation of 2-propanol (IPA).

Five Au NR samples with different aspect ratios (defined as length divided by width of the nanorod) were synthesized by seed-mediated synthetic route.[13] The plasmon resonance absorption splits into two modes corresponding to the oscillation of the free electrons along and perpendicular to the long axis of the rods. The transverse mode shows a resonance at about 520 nm, while the resonance of the longitudinal mode is red-shifted and strongly depends on aspect ratio of the nanorod (Supporting Information, Figure S1).[14] This is caused by charge accumulation difference along the rod axis (longitudinal plasma) and along a perpendicular direction (transversal plasma), and the charge accumulation will be maximum for the latter. As the restoring force is proportional to this charge accumulation, smaller forces and consequently smaller resonance frequencies are required for exciting longitudinal plasmon resonance. As can be seen from the TEM images (Supporting Information, Figure S2), Au NRs in five samples possess similar longitudinal length (ca. 40 nm), while different aspect ratios (ca. 1.8, 2.3, 2.7, 3.3, 4.0) were obtained with the decrease of transverse length. A lattice space measured as 0.204 nm, corresponding to Au (200) lattice plane, was easily discerned in HRTEM

[*] Dr. L. Q. Liu, Dr. S. X. Ouyang, Prof. J. H. Ye
International Center for Materials Nanoarchitectonics (WPI-MANA) and Environmental Remediation Materials Unit
National Institute for Materials Science (NIMS)
1-1 Namiki, Tsukuba, Ibaraki 305-0044 (Japan)
E-mail: jinhua.ye@nims.go.jp
Prof. J. H. Ye
TU-NIMS Joint Research Center
School of Material Science and Engineering
Tianjin University (P.R. China)

[**] This work received financial support from the World Premier International Research Center Initiative (WPI Initiative) on Materials Nanoarchitectonics, and MEXT (Japan).

Supporting information for this article is available on the WWW under http://dx.doi.org/10.1002/anie.201300239.

image, indicating good crystallinity of Au NRs. Au NR-loaded TiO_2 photocatalysts were prepared by impregnating colloidal gold nanorods with TiO_2 (5 μm in diameter). Calcination is not suitable in this case to remove bilayer surfactant adhere onto Au NRs as the morphology of colloidal gold nanorod will be destroyed by heating before the release of the inner layer surfactant.[15] Here, an oxidative method with $HClO_4$ is developed to remove this bilayer surfactant (see catalyst preparation in the Supporting Information). An Au NR-loaded TiO_2 photocatalyst with longitudinal plasmon resonance adsorption peak centered at 660 nm was prepared through the route mentioned above, denoted as Au NR/TiO_2-660, with the purpose of studying surfactant removal and morphology of Au NRs on TiO_2. The surfactant removal over Au NR/TiO_2-660 is verified by differential thermal analysis (DTA) spectra (Figure 1). Over as-prepared Au NR/TiO_2,

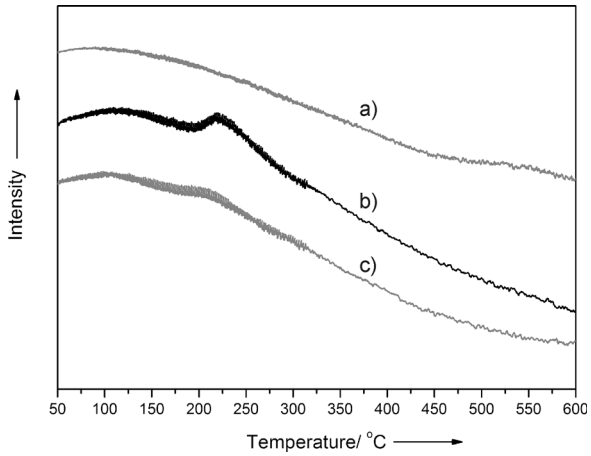

Figure 1. DTA curves of a) TiO_2 and b,c) Au NR/TiO_2-660 before (b) and after (c) $HClO_4$ oxidative treatment.

there is an obvious exothermic peak centered at 220 °C, corresponding to surfactant combustion with oxygen. This exothermic peak disappeared after the catalyst was treated with $HClO_4$, indicating at least most surfactant has been successfully removed. A slow endothermic peak tailed to higher temperature over Au NR/TiO_2-660 might be caused by desorption of adsorbents, which is similar to that of TiO_2. The morphology maintenance of Au NRs during $HClO_4$ treatment was studied by HAADF-STEM, HRTEM and diffusion reflectance spectrophotometer. As can be seen from Figure 2a and b, well dispersed gold nanorods (bright rods) can be discerned from the background. This assignment is confirmed by STEM-elemental mapping (Supporting Information, Figure S3). In HRTEM image, Figure 2c, Au NRs with an aspect ratio of 2.3 as well as TiO_2 crystals can be easily discerned. As compared with TEM and STEM images before $HClO_4$ treatment (Supporting Information, Figure S4), there is no significant change in morphology of Au NRs. This is in accordance with adsorption position maintenance in normalized diffusion reflectance spectra except for slight broadening (Supporting Information, Figure S5). More importantly, as shown in Figure 2d, a close contact is formed at the interface of Au NRs and TiO_2, which would facilitate the electron or

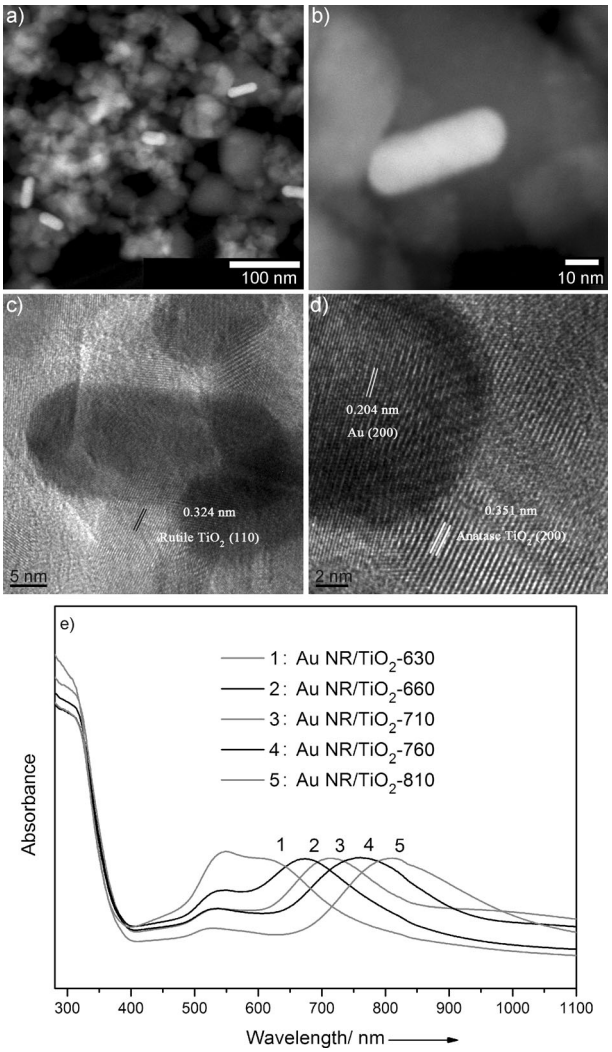

Figure 2. a,b) HAADF-STEM images and c,d) HRTEM images of the Au NR/TiO_2-660 photocatalyst; e) UV/Vis absorption spectra of Au NR/TiO_2 photocatalysts.

energy transfer in this composite photocatalyst. These studies indicate that $HClO_4$ oxidative method is an efficient method to remove surfactant over Au NRs without noticeably destroying its morphology. Five TiO_2-supported Au NR catalysts were prepared by loading Au NRs with different aspect ratios, and the surfactant was removed by the $HClO_4$ oxidative method. By adjusting the aspect ratio of Au NRs, longitudinal plasmon resonance adsorptions are tuned from 630 nm to 810 nm (Figure 2e). The corresponding catalysts are denoted as Au NR/TiO_2-630, Au NR/TiO_2-660, Au NR/TiO_2-710, Au NR/TiO_2-760, and Au NR/TiO_2-810. It should be pointed out that there is an overlap between transversal and longitudinal plasmon resonance adsorption in Au NR/TiO_2-630, which is mainly caused by the relative low aspect ratio (ca. 1.8) and slight transformation of nanorod to sphere during preparation procedure.[16] From XRD patterns (Supporting Information, Figure S6), Au (200), (220), and (311) diffraction planes can also be recognized along with characteristic anatase and rutile TiO_2 diffraction peaks, which agrees well with TEM results. Photocatalytic oxidation of IPA served

as a model reaction to evaluate the wavelength dependence photocatalytic activity over those photocatalysts. To identify the activity derived from transversal or longitudinal plasma of Au NRs, the reactions were carried out under different broadband light irradiation. That is, broadband light I: visible light cover transversal plasmon resonance of Au NRs only (ca. $400 < \lambda < 650$ nm; Supporting Information, Figure S7a); broadband light II: visible light cover both transversal and longitudinal plasmon resonance of Au NRs (ca. $400 < \lambda < 820$ or 910 nm; Supporting Information, Figure S7b). Details on catalyst preparation, characterization, and photocatalytic evaluation can be found in the Supporting Information.

Photocatalytic activity evaluation results under different reaction conditions are given in Table 1 and the Supporting Information, Table S1. Taking Au NR/TiO_2-660 and Au NR/TiO_2-710 for example, 12.0 μmol acetone and 0.61 μmol CO_2 were obtained over Au NR/TiO_2-660 under broadband light I irradiation for 10 h (Figure 3a). In contrast, only 0.12 μmol acetone and 0.08 μmol CO_2 were obtained under dark reaction carried out at 30 °C, which primarily indicated a visible-light photocatalytic activity was achieved by introducing Au onto TiO_2, as reported earlier.[17] Furthermore, this activity is enhanced by 2.8 times in terms of acetone production under broadband light I irradiation as compared with that of Au NR/TiO_2 without $HClO_4$ oxidative treatment (Table 1, Supporting Information, Figure S8), suggesting the removal of surfactant facilitate charge carriers or energy transfer in plasmonic composite photocatalysts. Dramatic activity increase was observed after increasing wavelength of light to cover not only transversal but also longitudinal plasmon resonance of Au NRs (broadband light II); that is, 75.0 μmol acetone and 19.7 μmol CO_2 were obtained. The enhancement factor (EF), calculated as the ratio of the IPA photooxidation rate R_{II} (under broadband light II irradiation) to R_I (under broadband light I irradiation), is as high as 6.6. This activity enhancement can be (at least roughly) ascribed to driving effect of longitudinal plasma of Au NRs. To further confirm the activity inspired from longitudinal plasma of Au NRs, plasmon-induced photooxidation was carried out under monochromic light irradiation at $\lambda = 660$ nm (Figure 3a inset). 1.1 μmol acetone and 0.15 μmol CO_2 were obtained, which are about 9 and 2 times, respectively, as many as that obtained under dark reaction. On the other hand, the IPA photooxidation rate over Au NR/TiO_2-660 under UV irradiation is about 1.8 times as high as that of TiO_2 (Supporting Information, Figure S9), which might be mainly caused by co-catalyst effect of the surface Au NRs.

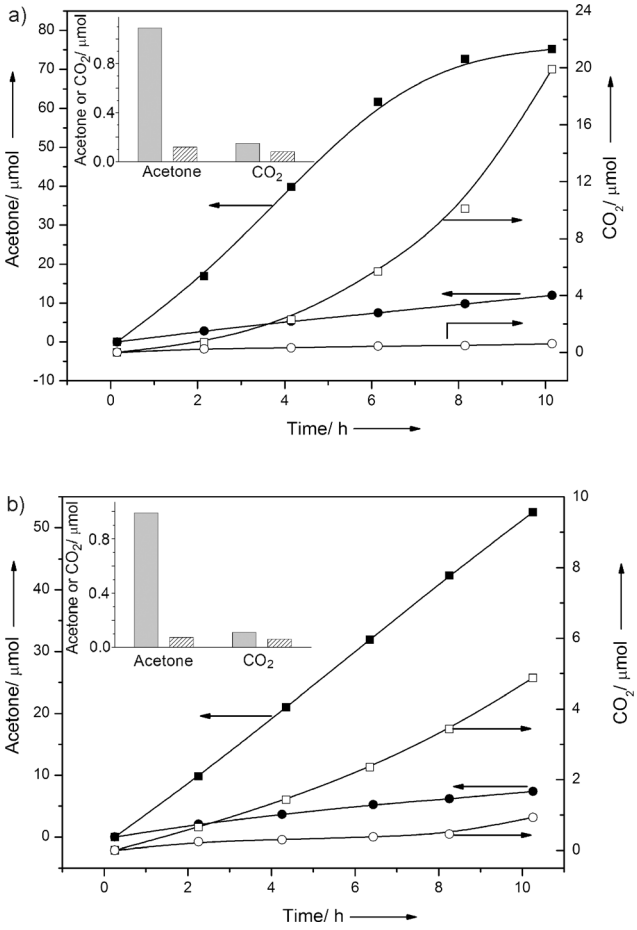

Figure 3. Curves of acetone (filled symbols) and CO_2 evolution (open symbols) in potocatalytic oxidation of IPA over Au NR/TiO2-660 (a) and over Au NR/TiO_2-710 (b) under broadband light I (●,○) and II (■,□) irradiation as a function of reaction time. Inset: reaction carried out under monochromic light irradiation for 10 h (gray: a) 660, b) 710 nm); shaded: dark reaction).

As for Au NR/TiO_2-710, 7.3 μmol acetone and 0.86 μmol CO_2 were obtained by irradiation under broadband light I for 10 h (Figure 3b). The photocatalytic activity induced by longitudinal plasma of Au NRs could also be clarified by comparing with the photocatalytic activity induced not only transversal but also longitudinal plasma of Au NRs; that is, 52.3 μmol acetone and 4.7 μmol CO_2 under broadband light II irradiation for 10 h with an EF of 7.1. Moreover, this activity is also higher than that of Au nanoparticles loaded TiO_2 (13.4 μmol acetone and 1.7 μmol CO_2; Supporting Information, Figure S10), further suggesting longitudinal plasma of

Table 1: Photocatalytic oxidation of 2-propanol (IPA) over Au NR-TiO_2 catalysts.

Catalyst	Au	Broadband I ($400 < \lambda < 650$ nm)[a,c]		Broadband II ($400 < \lambda < 820$ or 910 nm)[b,c]		Monochromatic light	
	Loading	Acetone	CO_2	Acetone	CO_2	Acetone	CO_2
Au NR-TiO_2-630	1.7	9.5	0.46	56.5	10.2	1.4	0.07
Au NR-TiO_2-660	1.5	12.0	0.61	75.0	19.7	1.1	0.15
Au NR-TiO_2-710	2.2	7.3	0.86	52.3	4.7	1.0	0.11
Au NR-TiO_2-760	2.6	18.3	0.45	62.5	26.5	1.2	0.12
Au NR-TiO_2-810	2.1	25.0	0.55	75.8	10.2	1.6	0.23
Au NR-TiO_2-660[d]	1.5	4.2	0.22	16.4	0.53	–	–

[a] Achieved by combining L42 + CM500S filters. [b] Achieved by combining L42 + R810 or R900 filters. [c] Photoreaction for 10 h, and the amounts of acetone and CO_2 have been subtracted with the corresponding values under dark reaction. [d] Au NR-TiO_2-660 before $HClO_4$ treatment. Units for acetone and CO_2 [μmol].

Au NRs are involved in photocatalytic oxidation of IPA. Though with higher gold loading, the activity over Au NR/TiO_2-710 is a little inferior to that of Au NR/TiO_2-660, indicating the photocalytic activity of Au NR/TiO_2 is not directly related to Au content. The ability to drive photocatalytic IPA oxidation by longitudinal plasma of Au NRs is also confirmed by reaction carried out under monochromic light irradiation at $\lambda = 710$ nm (Figure 3 b inset). Additionally, the catalyst after being irradiated under broadband light II for 10 h was characterized by UV/Vis diffusion reflectance spectrophotometer (Supporting Information, Figure S11). There is no significant change in the position of both transversal and longitudinal plasmon resonance adsorption, while the slight intensity increase of transversal plasmon resonance adsorption might be caused by transformation of trace gold nanorods to spheres through surface diffusion.[16b]

Over the other three catalysts, Au NR/TiO_2-630, Au NR/TiO_2-760, and Au NR/TiO_2-810, photocatalytic activities induced by longitudinal plasma of Au NRs are also identified by carrying out the reaction under irradiation of broadband light I and II, respectively (Supporting Information, Figures S12–14). Dramatic activity increases were achieved when irradiation covers both transversal and longitudinal plasmon resonance of Au NRs with EFs in the range of 3.1–6.2. It is worthy to point out that the enhancement effects decrease for Au NR/TiO_2-760 and Au NR/TiO_2-810 catalysts, which should be caused by the obvious light intensity decrease of Xe lamp in this near infrared region though broadband II were also extended in these two cases.[18] This result, in turn, indicates that this photocatalytic process, even under near-infrared light irradiation, is derived by longitudinal plasma of Au NRs. This assumption is further evidenced by reaction carried out under monochromc light irradiation. These results indicate that gold nanorods are the species responsible for light absorption and trigger the photochemical reactions. A comparison study and wavelength dependence activity give clear evidence that the IPA photooxidation can be driven by longitudinal plasma of Au NRs, which largely extends the light harvesting from about 520 nm of spherical Au particles to about 810 nm. Furthermore, Au NR/TiO_2 was subjected to photodegradation of aldehyde (Supporting Information, Figure S15). Aldehyde can also be photooxidized to CO_2 with long-wavelength visible-light irradiation, suggesting these Au NRs photosensitized catalysts seems to have a good universality.

Two main mechanisms have been proposed to explain the enhancement in photocatalytic activity in those composite systems compared to pure TiO_2. One is electron injection from Au to TiO_2 and the other is energy transfer from excited Au LSPR to TiO_2.[19] High intensity of LSPR is manifested as amplification effect for electromagnetic field in the vicinity of Au NRs as observed in Raman scattering[20] (Supporting Information, Figure S16). Meanwhile, it is suggested that the intensity of plasmon resonance of Au NRs is enhanced compared with that of sphere Au nanoparticles,[21] which agrees with the large activity enhancement induced by longitudinal plasma of Au NRs as compared with that of transversal plasma only. At this stage, charge carriers in TiO_2 with sufficient redox potentials excited by photons from Au NR LSPR decaying are proposed to account for the visible-light activities achieved over Au NR/TiO_2 in photocatalytic IPA oxidation, while the heating effect can be excluded in this case as it is characteristic of small particles.[22] Despite this analysis, the underlying physical mechanism is still obscure. Therefore, further study on this issue is required, which is import in developing effective plasmonic composite phototatalysts.

In summary, broadband visible and even near-infrared light harvesting over TiO_2 has been successfully achieved by introducing gold nanorods as antennas, while surfactant adhered onto the Au NR surface was successfully removed by an $HClO_4$ oxidative method without noticeably changing its morphology. Photocatalytic activities induced by not only transversal but also longitudinal plasma of gold nanorods were confirmed, and the broadband visible-light activities are speculated to be caused by LSPR of Au NRs. Moreover, the adjustable light adsorption resulting from the tunability of gold nanorod aspect ratio would benefit to designing photocatalyst with specific light harvesting. The strategy of introducing gold nanorods and surfactant removing by $HClO_4$ oxidative method reported here might open an avenue to develop broadband visible-light sensitive photocatalysts.

Received: January 11, 2013
Revised: April 8, 2013
Published online: May 10, 2013

Keywords: gold · photocatalysis · surface plasmon resonance · titania · visible light

[1] a) H. Tong, S. Ouyang, Y. Bi, N. Umezawa, M. Oshikiri, J. Ye, *Adv. Mater.* **2012**, *24*, 229 – 251; b) H. Zhou, Y. Qu, T. Zeid, X. Duan, *Energy Environ. Sci.* **2012**, *5*, 6732 – 6743.

[2] a) J. W. Tang, Z. G. Zou, J. H. Ye, *Angew. Chem.* **2004**, *116*, 4563 – 4566; *Angew. Chem. Int. Ed.* **2004**, *43*, 4463 – 4466; b) D. F. Wang, T. Kako, J. H. Ye, *J. Am. Chem. Soc.* **2008**, *130*, 2724 – 2725.

[3] A. Fujishima, K. Honda, *Nature* **1972**, *238*, 37 – 38.

[4] M. R. Hoffmann, S. T. Martin, W. Choi, D. W. Bahnemann, *Chem. Rev.* **1995**, *95*, 69 – 96.

[5] W. Choi, A. Termin, M. R. Hoffmann, *J. Phys. Chem.* **1994**, *98*, 13669 – 13679.

[6] a) R. Asahi, T. Morikawa, T. Ohwaki, K. Aoki, Y. Taga, *Science* **2001**, *293*, 269 – 271; b) S. U. M. Khan, M. Al-Shahry, W. B. Ingler, *Science* **2002**, *297*, 2243 – 2245; c) S. Sakthivel, H. Kisch, *Angew. Chem.* **2003**, *115*, 5057 – 5060; *Angew. Chem. Int. Ed.* **2003**, *42*, 4908 – 4911; d) W. J. Ren, Z. H. Ai, F. L. Jia, L. Z. Zhang, X. X. Fan, Z. G. Zou, *Appl. Catal. B* **2007**, *69*, 138 – 144; e) X. B. Chen, L. Liu, P. Y. Yu, S. S. Mao, *Science* **2011**, *331*, 746 – 750.

[7] a) E. Hutter, J. H. Fendler, *Adv. Mater.* **2004**, *16*, 1685 – 1706; b) S. Linic, P. Christopher, D. B. Ingram, *Nat. Mater.* **2011**, *10*, 911 – 921; c) A. Primo, A. Corma, H. Garcia, *Phys. Chem. Chem. Phys.* **2011**, *13*, 886 – 910; d) P. Wang, B. Huang, Y. Dai, M. H. Whangbo, *Phys. Chem. Chem. Phys.* **2012**, *14*, 9813 – 9825; e) W. Hou, S. B. Cronin, *Adv. Funct. Mater.* **2013**, *23*, 1612 – 1619.

[8] a) P. Wang, B. Huang, X. Qin, X. Zhang, Y. Dai, J. Wei, M. H. Whangbo, *Angew. Chem.* **2008**, *120*, 8049 – 8051; *Angew. Chem. Int. Ed.* **2008**, *47*, 7931 – 7933; b) Q. Zhang, D. Q. Lima, I. Lee, F. Zaera, M. F. Chi, Y. D. Yin, *Angew. Chem.* **2011**, *123*, 7226 –

7230; *Angew. Chem. Int. Ed.* **2011**, *50*, 7088 – 7092; c) H. M. Chen, C. K. Chen, C.-J. Chen, L.-C. Cheng, P. C. Wu, B. H. Cheng, Y. Z. Ho, M. L. Tseng, Y.-Y. Hsu, T.-S. Chan, J.-F. Lee, R.-S. Liu, D. P. Tsai, *ACS Nano* **2012**, *6*, 7362 – 7372; d) W. B. Hou, W. H. Hung, P. Pavaskar, A. Goeppert, M. Aykol, S. B. Cronin, *ACS Catal.* **2011**, *1*, 929 – 936; e) P. Christopher, H. Xin, A. Marimuthu, S. Linic, *Nat. Mater.* **2012**, *11*, 1044 – 1050; f) X. Chen, P. Li, H. Tong, T. Kako, J. Ye, *Sci. Technol. Adv. Mater.* **2011**, *12*, 044604.

[9] E. A. Coronado, E. R. Encina, F. D. Stefani, *Nanoscale* **2011**, *3*, 4042 – 4059.

[10] a) Z. W. Seh, S. Liu, S. Y. Zhang, M. S. Bharathi, H. Ramanarayan, M. Low, K. W. Shah, Y. W. Zhang, M. Y. Han, *Angew. Chem.* **2011**, *123*, 10322 – 10325; *Angew. Chem. Int. Ed.* **2011**, *50*, 10140 – 10143; b) R. Liu, A. Sen, *J. Am. Chem. Soc.* **2012**, *134*, 17505 – 17512.

[11] A. Antonello, E. Della Gaspera, J. Baldauf, G. Mattei, A. Martucci, *J. Mater. Chem.* **2011**, *21*, 13074 – 13078.

[12] a) Y. Q. Qu, R. Cheng, Q. Su, X. F. Duan, *J. Am. Chem. Soc.* **2011**, *133*, 16730 – 16733; b) J. Lee, S. Mubeen, X. Ji, G. D. Stucky, M. Moskovits, *Nano Lett.* **2012**, *12*, 5014 – 5019.

[13] C. J. Murphy, L. B. Thompson, A. M. Alkilany, P. N. Sisco, S. P. Boulos, S. T. Sivapalan, J. A. Yang, D. J. Chernak, J. Huang, *J. Phys. Chem. Lett.* **2010**, *1*, 2867 – 2875.

[14] S. Link, M. B. Mohamed, M. A. El-Sayed, *J. Phys. Chem. B* **1999**, *103*, 3073 – 3077.

[15] a) B. Nikoobakht, M. A. El-Sayed, *Langmuir* **2001**, *17*, 6368 – 6374; b) H. Petrova, J. P. Juste, I. Pastoriza-Santos, G. V. Hartland, L. M. Liz-Marzán, P. Mulvaney, *Phys. Chem. Chem. Phys.* **2006**, *8*, 814 – 821.

[16] a) J. Perezjuste, I. Pastorizasantos, L. Lizmarzan, P. Mulvaney, *Coord. Chem. Rev.* **2005**, *249*, 1870 – 1901; b) Y. Khalavka, C. Ohm, L. Sun, F. Banhart, C. Sonnichsen, *J. Phys. Chem. C* **2007**, *111*, 12886 – 12889.

[17] a) E. Kowalska, O. O. P. Mahaney, R. Abe, B. Ohtani, *Phys. Chem. Chem. Phys.* **2010**, *12*, 2344 – 2355; b) D. Tsukamoto, Y. Shiraishi, Y. Sugano, S. Ichikawa, S. Tanaka, T. Hirai, *J. Am. Chem. Soc.* **2012**, *134*, 6309 – 6315; c) F. J. López-Tenllado, A. Marinas, F. J. Urbano, J. C. Colmenares, M. C. Hidalgo, J. M. Marinas, J. M. Moreno, *Appl. Catal. B* **2012**, *128*, 150 – 158.

[18] D. B. Ingram, P. Christopher, J. L. Bauer, S. Linic, *ACS Catal.* **2011**, *1*, 1441 – 1447.

[19] a) Y. Tian, T. Tatsuma, *J. Am. Chem. Soc.* **2005**, *127*, 7632 – 7637; b) S. K. Cushing, J. Li, F. Meng, T. R. Senty, S. Suri, M. Zhi, M. Li, A. D. Bristow, N. Wu, *J. Am. Chem. Soc.* **2012**, *134*, 15033 – 15041.

[20] Q. J. Xiang, J. G. Yu, B. Cheng, H. C. Ong, *Chem. Asian J.* **2010**, *5*, 1466 – 1474.

[21] M. A. Garcia, *J. Phys. D* **2011**, *44*, 283001.

[22] a) D. D. Evanoff, G. Chumanov, *ChemPhysChem* **2005**, *6*, 1221 – 1231; b) X. Chen, H. Y. Zhu, J. C. Zhao, Z. F. Zheng, X. P. Gao, *Angew. Chem.* **2008**, *120*, 5433 – 5436; *Angew. Chem. Int. Ed.* **2008**, *47*, 5353 – 5356; c) S. Mukherjee, F. Libisch, N. Large, O. Neumann, L. V. Brown, J. Cheng, J. B. Lassiter, E. A. Carter, P. Nordlander, N. J. Halas, *Nano Lett.* **2013**, *13*, 240 – 247.

